TU/e EINDHOVEN UNIVERSITY OF TECHNOLOGY

Relationship Between Equilibrium Hydrogen Pressure and Exchange Current for the Hydrogen Electrode-Reaction at Mmni(3.9-X)Mn(0.4)A1(X)Co(0.7) Alloy Electrodes

Citation for published version (APA):
Senoh, H., Morimoto, K., Inoue, H., Iwakura, C., & Notten, P. H. L. (2000). Relationship Between Equilibrium Hydrogen Pressure and Exchange Current for the Hydrogen Electrode-Reaction at Mmni(3.9-X)Mn(0.4)A1(X)Co(0.7) Alloy Electrodes. *Journal of the Electrochemical Society*, *147*(7), 2451-2455. https://doi.org/10.1149/1.1393552

DOI:
10.1149/1.1393552

Document status and date:
Published: 01/01/2000

Document Version:
Publisher's PDF, also known as Version of Record (includes final page, issue and volume numbers)

Please check the document version of this publication:

• A submitted manuscript is the version of the article upon submission and before peer-review. There can be important differences between the submitted version and the official published version of record. People interested in the research are advised to contact the author for the final version of the publication, or visit the DOI to the publisher's website.
• The final author version and the galley proof are versions of the publication after peer review.
• The final published version features the final layout of the paper including the volume, issue and page numbers.

Link to publication

General rights
Copyright and moral rights for the publications made accessible in the public portal are retained by the authors and/or other copyright owners and it is a condition of accessing publications that users recognise and abide by the legal requirements associated with these rights.

• Users may download and print one copy of any publication from the public portal for the purpose of private study or research.
• You may not further distribute the material or use it for any profit-making activity or commercial gain
• You may freely distribute the URL identifying the publication in the public portal.

If the publication is distributed under the terms of Article 25fa of the Dutch Copyright Act, indicated by the "Taverne" license above, please follow below link for the End User Agreement:

www.tue.nl/taverne

Take down policy
If you believe that this document breaches copyright please contact us at:

openaccess@tue.nl

providing details and we will investigate your claim.

Download date: 04. Oct. 2023

Journal of The Electrochemical Society, **147** (7) 2451-2455 (2000)
S0013-4651(99)11-008-5 CCC: $7.00 © The Electrochemical Society, Inc.

Relationship Between Equilibrium Hydrogen Pressure and Exchange Current for the Hydrogen Electrode Reaction at $MmNi_{3.9-x}Mn_{0.4}Al_xCo_{0.7}$ Alloy Electrodes

Hiroshi Senoh,[a] Kohji Morimoto,[a] Hiroshi Inoue,[a] Chiaki Iwakura,[a,*,z] and P. H. L. Notten[b,c,*]

[a]*Department of Applied Chemistry, Graduate School of Engineering, Osaka Prefecture University, Sakai, Osaka 599-8531, Japan*
[b]*Philips Research Laboratories, 5656 AA Eindhoven, The Netherlands*
[c]*Eindhoven University of Technology, 5612 AZ Endhoven, The Netherlands*

We present a theoretical relationship between equilibrium hydrogen pressure and exchange current for the hydrogen electrode reaction which considers the degree of hydrogen coverage at the electrode surface. Electrochemical measurements at $MmNi_{3.9-x}Mn_{0.4}Al_xCo_{0.7}$ ($0 \leq x \leq 0.8$) electrodes were performed to prove the theoretical model. The equilibrium hydrogen pressures were analyzed from electrochemical pressure-composition isotherms, and the exchange currents were determined by linear polarization measurements. Fitting the experimental data to the theoretical model indicated that the rate constants for the charge-transfer reaction as well as the charge-transfer coefficient were influenced by the partial substitution of nickel by aluminum. Also, the exchange current passed through a maximum with decreasing equilibrium hydrogen pressure, *i.e.*, with increasing aluminum content, indicating that it is possible to design new materials which combine high electrocatalytic activity with an appropriate equilibrium hydrogen pressure. Because of its high energy density and high power density, $MmNi_{3.6}Mn_{0.4}Al_{0.3}Co_{0.7}$ was found to be the most appropriate composition.
© 2000 The Electrochemical Society. S0013-4651(99)11-008-5. All rights reserved.

Manuscript submitted November 2, 1999; revised manuscript received February 28, 2000.

Nickel-metal hydride (Ni-MH) batteries have attracted significant attention during the last decade because of their applications in consumer electronics, electric vehicles (EVs), and hybrid electric vehicles (HEVs). Research and development of the negative electrode materials are, however, still essential for further improvement of energy density, power density, and rate capability.[1,2]

The exchange current (density), I_0, for the hydrogen electrode reaction is one of the most important parameters for understanding electrode kinetics and is a measure of electrocatalytic activity of the negative electrode. The exchange current is influenced by changing the alloy composition, by mixing the alloy with other metals or oxides, or by adding chemical reducing agents to the electrolyte in order to activate the electrode surface.[3-7] Equations for the exchange current for metal hydride electrodes have been proposed by many research groups, and the electrode reaction mechanisms have been discussed extensively.[3,4,8-11]

Enyo and Maoka[8] investigated the detailed mechanism of the hydrogen electrode reaction by overpotential transients on a Pd hydrogen electrode and presented individual rates of the elementary steps and the activity of hydrogen adatoms on the electrode surface. Yayama *et al.*[9] proposed a simple theoretical model to describe the dependence of the equilibrium potential and exchange current on the hydrogen content of crystalline $TiMn_{1.5}H_x$. The experimental data could, however, only fit the model at low H content. Yang *et al.*[10] derived a modified model for this dependence and obtained several parameters, such as the equilibrium constant of the hydrogen transfer process, the maximum value of the storable hydrogen concentration, and the reaction order of the electrode reaction, from the fit of a model with no H-H interaction to Yayama's experimental data. Wakao and Yonemura[11] investigated the rate determining process in the electrode reaction on hydrogen-absorbing metal electrodes, such as $LaNi_{5-x}Al_x$, by anodic polarization measurements, and determined the charge-transfer coefficient for selected electrodes. Furthermore, one of the present authors[3,4] derived an expression for the exchange current involved in the electrochemical formation/decomposition process, by considering the influence of electrode blocking by adsorbed hydrogen.

The equilibrium hydrogen pressure (P_{H_2}) is another important parameter for hydrogen storage alloys to predict the electrochemical discharge capacity of the negative electrodes because the capacity could be calculated from the hydrogen storage capacity (H/M) between $P_{H_2} = 5$ and 0.1 atm from pressure-composition isotherm (PCT) curves at 45°C.[12] For high energy density and high power density of Ni-MH batteries, it is essential that the negative electrode material combines an appropriate plateau pressure with excellent electrocatalytic activity for the hydrogen electrode reaction. The purpose of the present study is to propose a theoretical model to define the relationship between the equilibrium hydrogen pressure and the exchange current and to prove its validity by experiments, using AB_5-type hydrogen storage electrodes. Moreover, from the as-obtained model parameters, the effect of partial substitution of Ni by Al on the reaction order of adsorbed hydrogen, charge-transfer coefficient, and reaction rate constants was investigated.

Theory

It has been shown that the hydrogen electrode reaction on the surface of AB_5-type hydrogen storage alloy in an alkaline solution proceeds via the Volmer-Tafel mechanism and not via the Heyrovsky reaction mechanism.[7,13,14] The hydrogen transfer across the metal interface into the absorption state should be included in the overall electrode process.[15] The following steps must be considered

$$H_2O + e^- \underset{k_a}{\overset{k_c}{\rightleftarrows}} H_{ad} + OH^- \quad [1]$$

Subsequently, two H_{ad} atoms can recombine, forming hydrogen molecules which desorb into the electrolyte and gas phase

$$2H_{ad} \rightleftarrows H_2(l) \quad [2]$$

$$H_2(l) \rightleftarrows H_2(g) \quad [3]$$

Alternatively, H_{ad} can be absorbed by the host material, according to

$$H_{ad} \rightleftarrows H_{abs} \quad [4]$$

The absorbed hydrogen (H_{abs}) can produce hydrogen gas in a cavity of the host material[16]

$$2H_{abs} \rightleftarrows H_2(m) \quad [5]$$

where k_c and k_a are the rate constants for the reduction and oxidation reaction. $H_2(l)$, $H_2(g)$, and $H_2(m)$ are hydrogen in the electrolyte, in the gas phase, and in the cavity of the host material, respectively. In the case of an AB_5-type hydrogen storage alloy, most of the H_{ad} dif-

* Electrochemical Society Active Member.
z E-mail: iwakura@chem.osakafu-u.ac.jp

Journal of The Electrochemical Society, 147 (7) 2451-2455 (2000)
S0013-4651(99)11-008-5 CCC: $7.00 © The Electrochemical Society, Inc.

fuses into the bulk of the alloy at a rate proportional to their concentration gradient.[17] In order to reduce the complexity of characterizing the kinetics of these reactions, it is assumed that hydrogen diffusion is sufficiently fast under certain conditions.

Under steady-state conditions in the absence of an external current, *i.e.*, when the Tafel reaction does not take place,[18] the configurational part of the chemical potential (μ_H) of H_{ad} is determined for an ideal, two-dimensional, randomly occupied surface lattice, by[19]

$$\mu_{H_{ad}} = \mu^{\circ}_{H_{ad}} + RT \ln \frac{\theta}{1-\theta} \quad [6]$$

where $\mu^{\circ}_{H_{ad}}$, R, T, and θ are the standard chemical potential of H_{ad}, the gas constant, absolute temperature, and the fraction of the electrode surface covered by H_{ad}, respectively. A similar relationship can be written for the chemical potential of $H_{2(m)}$ ($\mu_{H2(m)}$) based on the cavity pressure or the equilibrium hydrogen pressure for hydrogen storage alloy[20]

$$\mu_{H_{2(m)}} = \mu^{\circ}_{H_{2(m)}} + RT \ln \frac{P_{H_2}}{P^{ref}_{H_2}} \quad [7]$$

where $\mu^{\circ}_{H2(m)}$ and P^{ref}_{H2} are the standard chemical potential of $H_2(m)$, and the value of P_{H_2} in the reference state, respectively. If equilibrium is ultimately attained between H_{ad} and $H_2(m)$, the above chemical potentials become equal

$$2\mu_{H_{ad}} = 2\mu_{H_{abs}} = \mu_{H2(m)} \quad [8]$$

so that we obtain

$$2\mu^{\circ}_{H_{ad}} + 2RT \ln \frac{\theta}{1-\theta} = \mu^{\circ}_{H_{2(m)}} + RT \ln \frac{P_{H_2}}{P^{ref}_{H_2}} \quad [9]$$

which yields after rearrangement

$$\frac{\theta}{1-\theta} = \frac{1}{K_1}\sqrt{P_{H_2}} \quad [10]$$

hence

$$\theta = \frac{\sqrt{P_{H_2}}}{\sqrt{P_{H_2}} + K_1} \quad [11]$$

where K_1 is constant, according to

$$K_1 = \sqrt{P^{ref}_{H_2}} \exp\left(\frac{2\mu^{\circ}_{H_{ad}} - \mu^{\circ}_{H_{2(m)}}}{2RT}\right) \quad [12]$$

I_0 is an important parameter to evaluate the electrocatalytic activity for the hydrogen electrode reaction. Considering Eq. 1 at the equilibrium potential, it has been shown that the electrochemical charge-transfer kinetics can be quantified by the exchange current, according to[3,4]

$$I_0 = FA_0 k_a^{(1-\alpha)} k_c^{\alpha} \theta^{x(1-\alpha)} (1-\theta)^{\alpha} a_{OH^-}^{y(1-\alpha)} a_{H_2O}^{z\alpha} \quad [13]$$

where A_0 is the electrode surface area. a_{OH^-} and a_{H_2O} are the activities of OH^- and H_2O species, respectively, x, y, and z their corresponding reaction orders, α the charge-transfer coefficient, and F the Faraday constant. Assuming that the diffusion limitations of H_2O and OH^- in the electrolyte are negligible due to their high concentrations in 6 M KOH solution, these activities can be considered as constant. Consequently, I_0 depends only on A_0, k_c, k_a, α, and θ.

Introducing the equation for θ into Eq. 13 ultimately gives a more convenient expression for I_0 *vs.* P_{H_2}, *i.e.*

$$I_0 = FA_0K_2 \frac{\left(\sqrt{P_{H_2}}\right)^{x(1-\alpha)} K_1^{\alpha}}{\left(\sqrt{P_{H_2}} + K_1\right)^{[x(1-\alpha)+\alpha]}} a_{OH^-}^{y(1-\alpha)} a_{H_2O}^{z\alpha} \quad [14]$$

in which K_2 is $k_a^{(1-\alpha)}k_c^{\alpha}$

Experimental

AB_5-type hydrogen storage alloys with the composition $MmNi_{3.9-x}Mn_{0.4}Al_xCo_{0.7}$ ($0 \le x \le 0.8$) were prepared by arc melting under an Ar atmosphere. The alloy ingots were mechanically pulverized under Ar, and the powders were sieved down to 53 μm. Crystallographic characterization of the alloys was carried out by the same method as reported previously.[6] Pressure-composition isotherms for hydrogen absorption were determined via the gas phase, using Sieverts' method at 25°C.

Electrodes were prepared by mixing 0.1 g of the alloy powder with 0.3 g Cu powder. These mixtures were pressed into pellets at 8×10^3 kg cm^{-2} for 5 min at room temperature. The resulting pellets, of diam 13 mm were covered with Ni sheets (30 mesh) and soldered to Ni wires. The setup of the electrochemical cell was similar to that described in a previous paper.[21] A 6 M KOH solution was used as electrolyte, and all measurements were performed at 25°C. For initial electrode activation, charge-discharge cycles were repeated ten times, using an automated charge/discharge unit (Hokuto Denko, HJ-201M6). The electrodes were charged for 3.5 h at 100 mA g^{-1}, followed by an open-circuit period of 30 min. They were then discharged at 40 mA g^{-1} to a cutoff potential of −0.65 V *vs.* Hg/HgO.

After 10 cycles, the electrodes were charged at 100 mA g^{-1} for 15 min [depth of charge (DOC) = *ca.* 10%], followed by a rest period of 30 min to allow the electrodes to reach equilibrium. Subsequently, the equilibrium potentials (E_{eq}) of the electrodes were measured *vs.* the Hg/HgO reference electrode. A linear polarization test was carried out in the vicinity of the equilibrium potential (±10 mV) at a scan rate of 1 mV s^{-1}. AC impedance measurements were carried out in the frequency range of 10 kHz to 0.01 Hz with the perturbation of 10 mV. The electrode was kept at the equilibrium potential during the AC impedance measurements.[22] These measurements were repeated after every 15 min charging period (DOC was changed in steps of *ca.* 10%) until the negative electrodes were fully charged. The measured potential range was from −0.65 to *ca.* −0.95 V *vs.* Hg/HgO.

The P_{H_2} values were calculated from the measured equilibrium potentials at 25°C, according to[4,23]

$$E_{eq}(V \text{ vs. Hg/HgO}) = -0.9310 - 0.0296 \log P_{H_2} \quad [15]$$

I_0 values were also obtained from the slope of the linear polarization (I/η) curves, according to[3]

$$I_0 = \frac{I}{\eta}\frac{RT}{F} \quad [16]$$

The impedance spectra were fitted to an equivalent circuit using a nonlinear least-squares fit program EQIVCT.[24]

Results and Discussion

The effect of Al content on the crystallographic structure of $MmNi_{3.9-x}Mn_{0.4}Al_xCo_{0.7}$ alloys was determined by X-ray diffraction (XRD). The XRD patterns showed that all alloys crystallized in the hexagonal $CaCu_5$ structure and that a second phase was rarely observed, indicating that all alloys in the present study had a homogeneous composition. From the spectra, the unit cell volume (V) was calculated. The results indicated that V increased steadily with increasing Al content. This is in agreement with generally adopted geometric considerations[25] because the atomic radius of Al (1.42 Å) is significantly larger than that of Ni (1.24 Å).

The surface areas of $MmNi_{3.9-x}Mn_{0.4}Al_xCo_{0.7}$ electrodes were changed appreciably by pulverization of the alloys during the initial activation. In order to activate the electrodes fully 10 activation cycles were carried out before the electrochemical measurements were performed. The discharge capacities of $MmNi_{3.9-x}Mn_{0.4}Al_xCo_{0.7}$ electrodes are shown in Fig. 1 as a function of cycle number. Each electrode reached its maximum discharge capacity within a few cycles, and the $MmNi_{3.6}Mn_{0.4}Al_{0.3}Co_{0.7}$ electrode was found to exhibit the best electrochemical characteristics in the present study. The electrode surface areas were determined by measuring the double layer capacitance by ac impedance spectroscopy, as mentioned later.

S0013-4651(99)11-008-5 CCC: $7.00 © The Electrochemical Society, Inc.

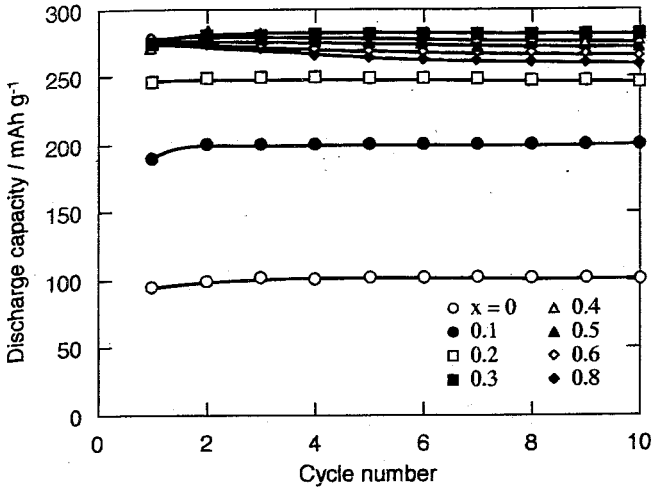

Figure 1. Activation profiles of $MmNi_{3.9-x}Mn_{0.4}Al_xCo_{0.7}$ electrodes at 25°C.

Figure 2 shows a comparison of the electrochemically determined PCT curves for hydrogen absorption in the various alloys at 25°C and those determined by gas phase measurements (Sieverts' method). The electrochemically measured PCT curves are in good agreement with those measured by Sieverts' method, indicating the validity of P_{H_2} evaluation by the electrochemical method.[4,23] Moreover, in the low P_{H_2} region, the electrochemical method is more effective than the gas phase method. Additionally, as can be concluded from Fig. 2, partial substitution of Ni by Al leads to a substantial decrease of hydrogen pressure. This is in accordance with the fact that the stability of the hydrides increases with increasing unit cell volume of the host material. Furthermore, increasing the Al content in the alloy results in an increased slope, suggesting a contraction of the α-to-β phase transition region.[25]

The dependencies of I_0 on the DOC are shown in Fig. 3 for all electrodes. In the low DOC region, the slope of the I_0 *vs.* DOC plots changes from negative to positive with increasing Al content. On the other hand, the I_0 values in the high DOC region are nearly independent of DOC for all electrodes. Considering the maximum I_0 values for each material, it is remarkable that I_0 first increases at lower Al content (see upper part of Fig. 3) then successively decreases at higher Al content (see lower part of Fig. 3). The maximum level is found for the $Al_{0.3}$ compound.

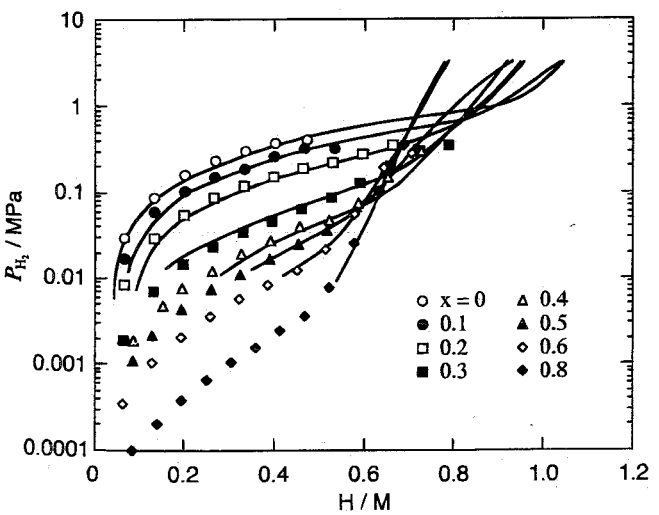

Figure 2. Pressure-composition isotherms for hydrogen absorption in $MmNi_{3.9-x}Mn_{0.4}Al_xCo_{0.7}$ alloy-hydrogen systems at 25°C measured by Sieverts' method (solid lines) and electrochemical method (symbols). The measured potential range was from −0.65 V to *ca.* −0.95 V *vs.* Hg/HgO.

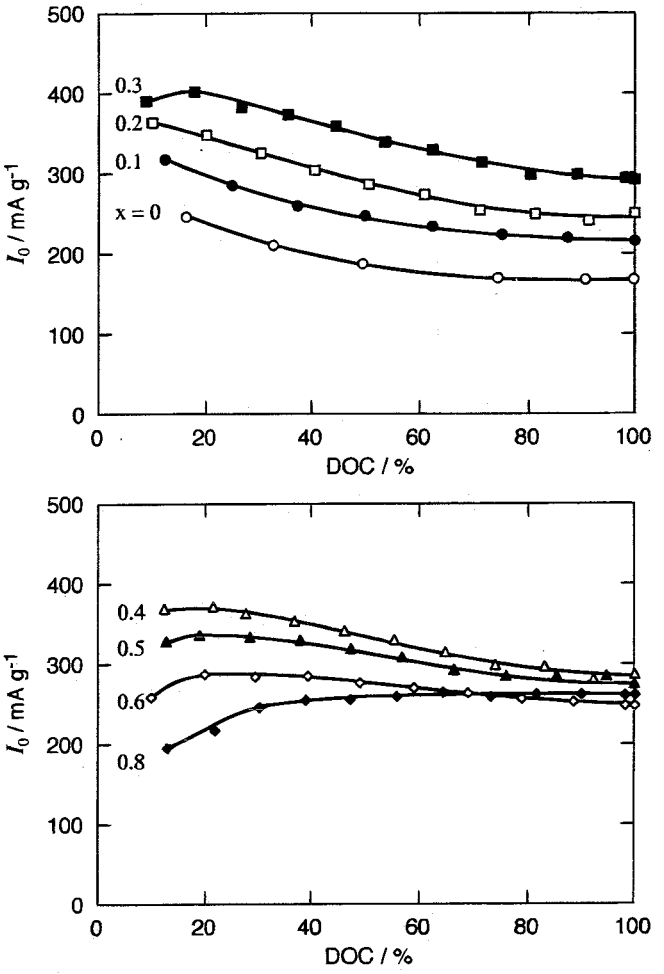

Figure 3. Exchange current as a function of depth of charge (DOC) for $MmNi_{3.9-x}Mn_{0.4}Al_xCo_{0.7}$ electrodes at 25°C.

The relationships between the electrochemically determined I_0 and P_{H_2} values are shown in Fig. 4. Strikingly, I_0 changes with increasing P_{H_2} for each electrode. In general, from the viewpoint of high energy density and high power density, an ideal negative electrode material combines an appropriate P_{H_2} value of about 0.01 MPa with a high I_0 value. $MmNi_{3.6}Mn_{0.4}Al_{0.3}Co_{0.7}$ appears to be the optimum composition in the present study.

In order to account for the experimental exchange current dependence on the equilibrium hydrogen pressure, Eq. 14 was used to generate the theoretical dependency. The parameters used in the simulations are given in Table I. The a_{OH^-} and a_{H_2O} values in 6 M KOH at 25°C and the reaction orders of OH^- and H_2O, y, and z, were obtained from the literature.[26,27] The value for A_0 was obtained from ac impedance measurement as follows.

The double layer capacitance (C_{dl}) is generally considered as a measure for the electrode surface area (A_0) in contact with the electrolyte. Therefore, the capacitance was determined by ac impedance spectroscopy for all electrode materials at various DOC. The electrochemical impedance spectra for a $MmNi_{3.6}Mn_{0.4}Al_{0.3}Co_{0.7}$ electrode measured from 10 kHz to 0.01 Hz are, as an example, shown in Fig. 5. As can be seen from this figure, each spectrum consists of small and large semicircles. The large semicircle clearly increases with DOC, indeed revealing an increase of the charge-transfer resistance. This is in agreement with the observed decrease in I_0 at high DOC (see Fig. 3). Between the large and small semicircles, short linear regions are observed over a limited frequency region for all spectra. This may be attributed to the distribution of reacting species through the porous electrodes[28,29] or to the contact resistance between the alloy particles in the pellet.[30] On the other hand, an ap-

Journal of The Electrochemical Society, **147** (7) 2451-2455 (2000)
S0013-4651(99)11-008-5 CCC: $7.00 © The Electrochemical Society, Inc.

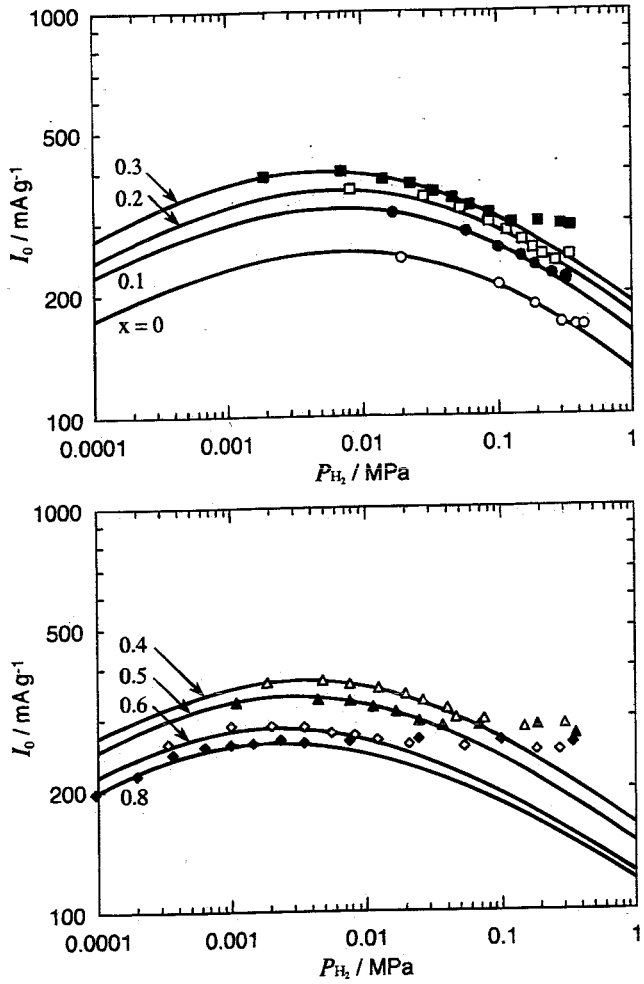

Figure 4. Exchange current as a function of equilibrium hydrogen pressure (symbols) for $MmNi_{3.9-x}Mn_{0.4}Al_xCo_{0.7}$ electrodes at 25°C. Theoretical curves (solid lines) are drawn based on the simulations described in the text.

proximate straight-line behavior in the low-frequency region corresponds to the spherical diffusion into the particles.[31] In the present study, a simplified equivalent circuit[32] was used to fit the impedance spectra and to evaluate the C_{dl} values. The as-analyzed C_{dl} values were approximately constant and independent of DOC, indicating that the change of I_0 with DOC, as shown in Fig. 3, is not influenced by A_0. Figure 6 shows the effect of Al content on C_{dl} for fully charged electrodes. The C_{dl} values are found to be constant, irrespective of Al content, indicating that the activated electrodes in the present study have identical surface areas. From Fig. 6 an average A_0 value of 7.4 m^2 g^{-1} was determined, assuming a double layer capacitance of 20 μF cm^{-2}.[33]

By using the parameters listed in Tables I and by optimizing the values of x, α, K_1, and K_2 in Eq. 14, the influence of P_{H_2} on I_0 was simulated for all electrodes. The results are represented in Fig. 4 by the solid lines. The theoretical curves are in quite good agreement with

Table I. The parameters used in the simulation.

Property	Symbol	Value
Faraday constant	F	96485 (C mol^{-1})
Specific surface area	A_0	7.4 (m^2 g^{-1})
Activity of OH^-	a_{OH^-}	10.4 (mol l^{-1})
Activity of H_2O	a_{H_2O}	0.649 (mol l^{-1})
Reaction orders of OH^- and H_2O	y, z	1, 1

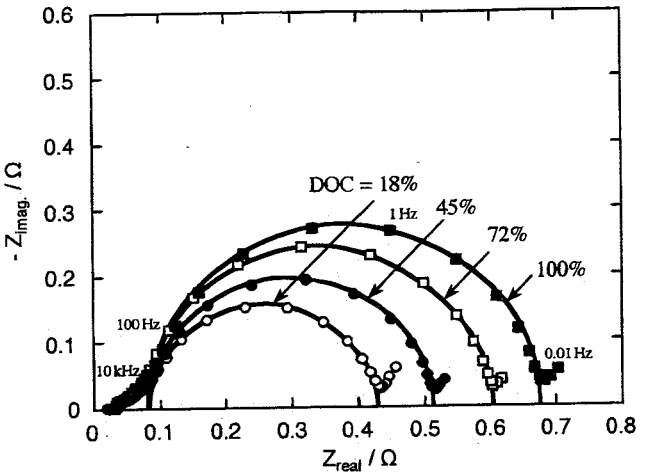

Figure 5. Impedance spectra for a $MmNi_{3.6}Mn_{0.4}Al_{0.3}Co_{0.7}$ electrode at various depths of charge (DOC). Solid lines are simulated results.

experimental values for all electrodes, indicating the validity of Eq. 14 for these multicomponent hydrogen storage alloys. The exchange currents show experimentally and theoretically a maximum with equilibrium hydrogen pressure for all electrodes. This indicates that it is, in principle, possible to design materials which combine an increase of electrocatalytic activity with a lower partial hydrogen pressure. The present results also indicate that the $MmNi_{3.6}Mn_{0.4}Al_{0.3}Co_{0.7}$ alloy not only has the highest electrocatalytic activity but also has a large hydrogen storage capacity. Some deviations are, however, observed but only at higher pressures. The explanation for this behavior must be involved in the phase transformation occurring at higher H content, implying that outside the solid-solution region Eq. 14 no longer holds. In addition, a nonequilibrium state at higher hydrogen pressures may play a role in the present experimental open-cell configuration.

From the simulations, a unique combination of four parameters in Eq. 14 was obtained for each electrode. The most reasonable value of reaction order for H_{ad} (x) was found to be unity for all electrodes. Yayama *et al.* have reported a value of 0.67 for the $TiMn_{1.5}$ system.[9] However, this value did not fit the present experimental results. The other parameters are summarized in Table II. From this table, it can be concluded that α assumes a reasonable value for all electrodes, which is similar to those measured at $LaNi_{5-x}Al_x$ electrodes by anodic polarization.[11] α decreases with increasing Al content, suggesting that the effective contribution of the overpotential to the hydrogen electrode reaction is changed by changing the Ni content in the alloy. The

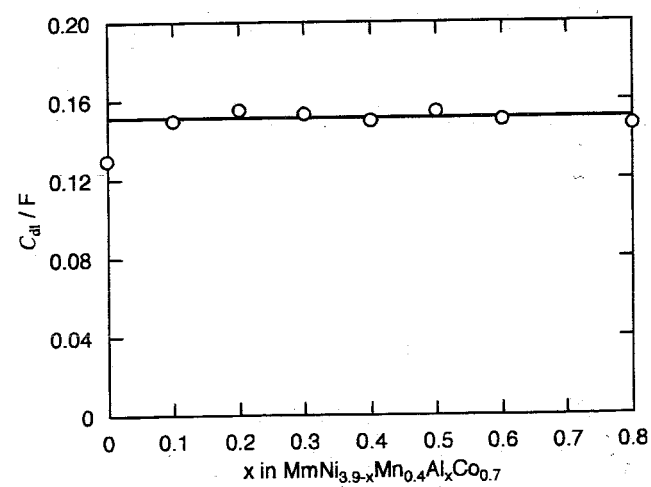

Figure 6. Effect of Al content on the double layer capacitance (C_{dl}) measured by ac impedance method at fully charged $MmNi_{3.9-x}Mn_{0.4}Al_xCo_{0.7}$ electrodes.

S0013-4651(99)11-008-5 CCC: $7.00 © The Electrochemical Society, Inc.

Table II. The charge-transfer coefficient α, parameters K_1, K_2 of Eq. 14 for $MmNi_{3.9-x}Mn_{0.4}Al_xCo_{0.7}$ ($0 \le x \le 0.8$) electrodes.

x	α	K_1	$K_2 \times 10^{-11}$ (cm s^{-1})
0	0.66	0.170	4.1
0.1	0.63	0.149	4.9
0.2	0.61	0.134	5.1
0.3	0.57	0.091	5.2
0.4	0.54	0.070	4.6
0.5	0.52	0.060	3.9
0.6	0.49	0.043	3.0
0.8	0.40	0.032	2.1

equilibrium constant for the hydrogen absorption process, K_1, is below unity, indicating that hydrogen is more easily transferred from the absorbed into the adsorbed state. The decrease of K_1 with increasing Al content indicates that hydrogen absorption becomes more inhibited. This is in agreement with the higher stability of these hydrides, as can also be concluded from the much lower equilibrium hydrogen pressures found for these materials (Fig. 2). The stabilization of the hydrides is due to the partial substitution of Ni by Al, which expands the unit cell. K_2, which is directly proportional to the I_0 value (see Eq. 14), increases at low Al content, but decreases above an Al content of 0.3. This is in agreement with Fig. 4. It should be noted that it is impossible to determine k_c and k_a independently from the present results and that K_2 may be influenced somewhat by the α value.

The theoretical relationship between I_0 and θ, as represented in Eq. 13, is shown in Fig. 7 for all electrodes. Based on the experimental data of P_{H_2} (see Fig. 2), the θ value was determined by using Eq. 11 and also shown in Fig. 7 by the symbols. The I_0 values show theoretically and experimentally a maximum when θ is about 0.5, *i.e.*, when half of the electrode surface is covered with adsorbed hydrogen. Considering the theoretical implications of Eq. 13, this is indeed to be expected with α values close to 0.5 (see Table II).[34] The surface coverage at which the alloy is converted into the β-phase is about 0.8. This value is independent of Al content. Obviously, for the θ values larger than 0.5, I_0 decreases. This means that the adsorbed hydrogen blocks the electrode surface, inhibiting the electrode charge-transfer reaction.

Conclusions

A model which reveals the importance of the relationship between the equilibrium hydrogen pressure and the exchange current for metal hydride electrode materials is presented. Using homogeneous $MmNi_{3.9-x}Mn_{0.4}Al_xCo_{0.7}$ electrode materials, in which x was varied between 0 and 0.8, this dependence was verified experimentally. The double layer capacitance of these electrodes, as determined by ac impedance spectroscopy, was found to be constant, irrespective of composition and depth of charge, indicating a constant electrode surface area. The equilibrium hydrogen pressures and the exchange currents were determined experimentally by electrochemical PCT and linear polarization measurements, respectively, and were found to be in good agreement with the theoretically derived relationship. Reaction rate constants and electrochemical parameters were obtained via simulations. The present model is, however, restricted to the solid-solution region. Outside this region other relationships must be taken into account, as will be outlined in a forthcoming paper.[35] Strikingly, both the simulations and experimental data indicate that the exchange current passes through a maximum with increasing equilibrium hydrogen pressure, indicating that it is, in principle, possible to design new materials which combine improved electrocatalytic activity with low partial hydrogen pressure. An alloy with composition $MmNi_{3.6}Mn_{0.4}Al_{0.3}Co_{0.7}$ has both an appropriate equilibrium hydrogen pressure and high electrocatalytic activity.

Osaka Prefecture University assisted in meeting the publication costs of this article.

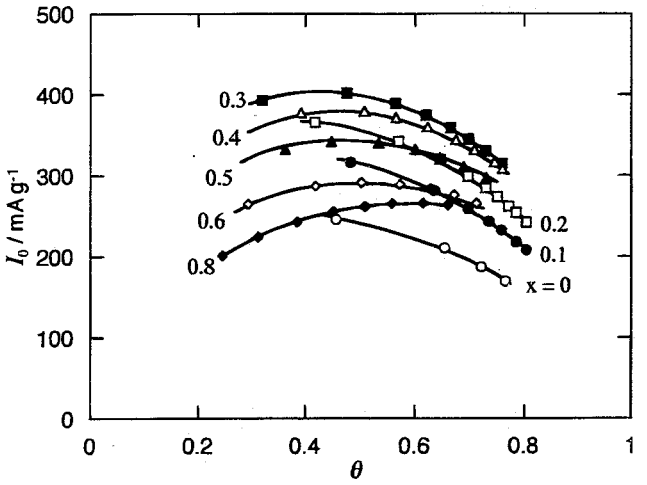

Figure 7. Exchange current as a function of the surface coverage by adsorbed hydrogen for $MmNi_{3.9-x}Mn_{0.4}Al_xCo_{0.7}$ electrodes at 25°C. Symbols were determined based on the experimental data of P_{H_2} (see Fig. 2) by using Eq. 11.

References

1. C. Iwakura and M. Matsuoka, *Prog. Batteries Battery Mater.*, **10,** 81 (1991).
2. T. Sakai, M. Matsuoka, and C. Iwakura, in *Handbook on the Physics and Chemistry of Rare Earths,* Vol. 21, K. A. Gschneidner, Jr. and L. Eyring, Editors, p. 133, Elsevier Science B.V., Amsterdam (1995).
3. P. H. L. Notten and P. Hokkeling, *J. Electrochem. Soc.*, **138,** 1877 (1991).
4. P. H. L. Notten, in *Interstitial Intermetallic Alloys,* NATO ASI Series E: Applied Science, Vol. 281, p. 151, F. Grandjean, G. J. Long, and K. H. J. Buschow, Editors, Kluwer Academic Publishers, London (1995).
5. T. Kitamura, C. Iwakura, and H. Tamura, *Chem. Lett.*, 965 (1981).
6. C. Iwakura, M. Matsuoka, K. Asai, and T. Kohno, *J. Power Sources,* **38,** 335 (1992).
7. C. Iwakura, M. Matsuoka, and T. Kohno, *J. Electrochem. Soc.*, **141,** 2306 (1994).
8. M. Enyo and T. Maoka, *J. Electroanal. Chem.*, **108,** 277 (1980).
9. H. Yayama, K. Hirakawa, and A. Tomokiyo, *Jpn. J. Appl. Phys.*, **25,** 739 (1986).
10. Q. M. Yang, M. Ciureanu, D. H. Ryan, and J. O. Ström-Olsen, *Electrochim. Acta,* **40,** 1921 (1995).
11. S. Wakao and Y. Yonemura, *J. Less-Common Met.*, **89,** 481 (1983).
12. H. Ogawa, M. Ikoma, K. Kawano, and I. Matsumoto, *J. Power Sources,* **12,** 393 (1989).
13. T. Kitamura, C. Iwakura, and H. Tamura, *Electrochim. Acta,* **27,** 1729 (1982).
14. K. Machida, M. Enyo, G. Adachi, and J. Shiokawa, *Electrochim. Acta,* **29,** 807 (1984).
15. S. Y. Qian, B. E. Conway, and G. Jerkiewicz, *J. Chem. Soc., Faraday Trans.*, **94,** 2945 (1998).
16. T. Maoka and M. Enyo, *Electrochim. Acta,* **26,** 607 (1981).
17. C. Iwakura, M. Miyamoto, H. Inoue, M. Matsuoka, and Y. Fukumoto, *J. Electroanal. Chem.*, **411,** 109 (1996).
18. Q. M. Yang, M. Ciureanu, D. H. Ryan, and J. O. Ström-Olsen, *J. Electrochem. Soc.*, **141,** 2108 (1994).
19. B. E. Conway and G. Jerkiewicz, *J. Electroanal. Chem.*, **357,** 47 (1993).
20. M. Enyo, *Electrochim. Acta,* **18,** 155 (1973).
21. C. Iwakura, K. Fukuda, H. Senoh, H. Inoue, M. Matsuoka, and Y. Yamamoto, *Electrochim. Acta,* **43,** 2041 (1998).
22. C. Iwakura, T. Oura, H. Inoue, and M. Matsuoka, *Electrochim. Acta,* **41,** 117 (1996).
23. C. Iwakura, T. Asaoka, H. Yoneyama, T. Sakai, K. Oguro, and H. Ishikawa, *Nippon Kagaku Kaishi,* 1482 (1988).
24. B. A. Boukamp, *Solid State Ionics,* **20,** 31 (1986).
25. P. H. L. Notten, M. Latroche, and A. Percheron-Guégan, *J. Electrochem. Soc.*, **146,** 3181 (1999).
26. H. Yayama, K. Kuroki, K. Hirakawa, and A. Tomokiyo, *Mem. Fac. Eng. Kyushu Univ.*, **57,** 801 (1984).
27. J. Balej, *Int. J. Hydrogen Energy,* **10,** 365 (1985).
28. M. Keddam, C. Rakotomavo, and H. Takenouti, *J. Appl. Electrochem.*, **14,** 437 (1984).
29. W. Zheng, M. P. S. Kumar, S. Srinivasan, and H. J. Ploehn, *J. Electrochem. Soc.*, **142,** 2935 (1995).
30. N. Kuriyama, T. Sakai, H. Miyamura, I. Uehara, H. Ishikawa, and T. Iwasaki *J. Electrochem. Soc.*, **139,** L72 (1992).
31. L. O. Valøen, S. Sunde, and R. Tunold, *J. Alloys Compd.*, **253-254,** 656 (1997).
32. R. D. Armstrong and M. Henderson, *J. Electroanal. Chem.*, **39,** 81 (1972).
33. A. Lasia and D. Gregoire, *J. Electrochem. Soc.*, **142,** 3393 (1995).
34. W. S. Kruijt, H. J. Bergveld, and P. H. L. Notten, *J. Electrochem. Soc.*, **145,** 3764 (1998).
35. H. Senoh, K. Morimoto, H. Inoue, C. Iwakura, and P. H. L. Notten, *Electrochemistry,* In preparation.